ChemComm
Chemical Communications

Accepted Manuscript

This article can be cited before page numbers have been issued, to do this please use: L. Chen, Y. Chen, W. Zhou, J. Li, Y. Zhang and Y. Liu, *Chem. Commun.*, 2020, DOI: 10.1039/D0CC01868F.

ROYAL SOCIETY OF CHEMISTRY

rsc.li/chemcomm

View Article Online
DOI: 10.1039/D0CC01868F

Journal Name

COMMUNICATION

Mitochondrial-targeted Chemiluminescent Ternary Supramolecular Assembly for in situ Photodynamic Therapy

Received 00th January 20xx,
Accepted 00th January 20xx

DOI: 10.1039/x0xx00000x

www.rsc.org/

Lei Chen, Yong Chen, Weilei Zhou, Jingjing Li, Yi Zhang and Yu Liu*

Smart supramolecular self-assembly for photodynamic therapy (PDT) and organelle targeting cell imaging has become a research hotspot due to fast and intelligent response. Herein, we report a novel ternary supramolecular assembly of nanoparticles. Overexpressed hydrogen peroxide in tumor cells rapidly stimulates the supermolecular nanoparticles to produce chemiluminescence and simultaneously sensitizes oxygen molecules to singlet oxygen ($^1O_2$) for in situ PDT. The supramolecular aggregated nanoparticle composed of photosensitizer molecules 4, 4'-(dibenzo [a, c] phenazine-9, 14-diyl) pyridin-1-ium bromide (DPAC-S) and cucurbit[7]uril (CB[7]), and co-assembly with bis [2, 4, 5-trichloro-6- (pentyloxycar-bonyl) phenyl] oxalate (CPPO). Cell imaging experiment further confirmed that nanoparticle assembly can effectively target mitochondria, which is beneficial to enhance PDT.

Differentiating from chemotherapy, surgery and radiotherapy, photodynamic therapy (PDT) is a minimally invasive and highly space-selective treatment for tumors.[1] This type of treatment requires three components to be effective. Oxygen, photosensitizers and light sources are the three primary components. Under selected light irradiation, the photosensitizer molecule is excited to the excited singlet state (S1), which can be filled into triplet states (T1) through intersystem crossing. Then the energy is transferred to the triplet oxygen molecule and produces free radicals and/or reactive oxygen species to damage adjacent cell.[2] The principal advantage of PDT is its high spatial selectivity, which originates from photosensitizer molecules that can only be excited under the selected wavelength of light.[3] Like other therapies, PDT has its limitation that it cannot treat deep tissue since light does not penetrate far away due to absorption and scattering of biological tissue.[1c,4] Near-infrared light can effectively overcome this problem, but the design of photosensitizer molecules for near-infrared absorption remains a challenge.[5] It is necessary to design a scheme that can release the limitation of PDT caused by external light source.

Chemiluminescence as tissue-penetration-depth-independent light is an effective way to solve the limitation of PDT caused by external light sources.[6] Chemiluminescence is a process of light radiation caused by the release of energy from chemical reactions usually between high-energy compound and hydrogen peroxide (H_2O_2).[7] Coincidentally, cancer cells exhibit high levels of H_2O_2 (ranging from 0.1 to 1 mM) compared to normal tissue cells (~10^{-4} mM).[8] Microenvironment of high concentration H_2O_2 endows chemiluminescence with regional specificity in tumors. Recently, a PDT system for in situ chemiluminescence and internal activation of photosensitizers was developed by Wang's team using luminol–H_2O_2–horseradish peroxidase system, which can kill adjacent cancer cells by stimulating photosensitizer molecules to produce reactive oxygen species through the bio-luminescence resonance energy transfer (BRET) process.[8b] Liu's team has constructed a new type of nanoparticles by wrapping bis [2, 4, 5-trichloro-6- (pentyloxycar-bonyl) phenyl] oxalate (CPPO) and photosensitizer molecule TBD in F-127 and soybean oil. As a unique H_2O_2 probe, these nanoparticles can image tumor tissues by chemiluminescence and produce reactive oxygen species to induce apoptosis of tumor cells[9]. However, supramolecular assembly platforms formed by macrocyclic host molecules and guest molecules can efficiently load hydrophobic drug molecules, as can CPPO molecules.[10] Such reports are still rare. Herein, we constructed supramolecular nanoparticles with chemiluminescence performance and in situ singlet oxygen ($^1O_2$) generation through the host-guest interaction in aqueous solution. Such nanoparticles have the following advantages: 1) CPPO is loaded into the assembly so that it can be water-soluble, so it can react with H_2O_2 quickly; 2) the assembly can effectively target the mitochondria in cells, enhancing the effect of PDT; 3) supramolecular assembly has good biocompatibility and little damage to normal tissue cells.

College of Chemistry, State Key Laboratory of Elemento-Organic Chemistry, Nankai University, Tianjin 300071, P. R. China. E-mail: yuliu@nankai.edu.cn

† Electronic Supplementary Information (ESI) available: Detailed synthesis, characterization data, Job's plots, association constants, absorption spectra and transmission electron microscopy images. See DOI: 10.1039/x0xx00000x

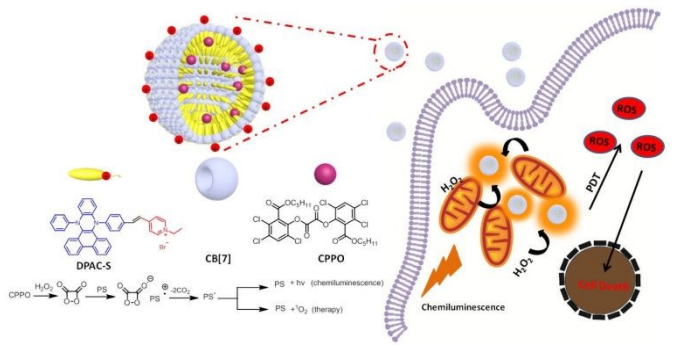

Scheme 1. Composition of supramolecular assemblies and schematic diagrams of photodynamic therapy and cellular imaging

Chemiluminescent supramolecular aggregated nanoparticle for effective PDT and chemiluminescence in tumor cell is illustrated in Scheme 1. 4, 4'-(dibenzo[a,c]phenazine-9,14-diyl) pyridin-1-ium bromide (DPAC-S) was synthesized according to literature (Figure S1, S2, S3).[11] DPAC-S and cucurbit[7]uril (CB[7]) can self-assemble into supramolecular assembly in aqueous solution through host-guest interaction.[12] As a hydrophobic molecule, CPPO co-assembly with the hydrophobic layer of supramolecular assembly to form supramolecular aggregated nanoparticle (DPAC-S@CB[7]@CPPO) with chemiluminescent properties.[13] When DPAC-S@CB[7]@CPPO interacts with cancer cells, water-soluble supramolecular aggregated nanoparticle can enter cells through endocytosis.[14] The pyridinium salt part of the DPAC-S makes the supramolecular aggregated nanoparticle positively charged, which enables the nanoparticle to target the mitochondria.[15] CPPO in DPAC-S@CB[7]@CPPO can interact with H_2O_2 released by mitochondria and produce energy. This part of the energy is efficient absorbed by the nearby guest molecule, which makes the guest molecule produce fluorescence emission. Guest molecule DPAC-S has been found to be an efficient photosensitizer molecule, so it can generate $^1O_2$ rapidly in suit while producing chemiluminescence. Ultimately, the DPAC-S@CB[7]@CPPO performed effective PDT in cancer cells without exposure to external light sources.

The guest molecule DPAC-S can bond effectively with the macrocyclic molecule cucurbituril due to the positively charged pyridine salt part. At first, DPAC-S was self-assembled with cucurbit[6]uril (CB[6]), cucurbit[7]uril (CB[7]) and cucurbit[8]uril (CB[8]). The results of scanning electron microscopy (SEM) and transmission electron microscopy (TEM) show that only CB[7] can form stable and regular nanoparticles with DPAC-S (Figure S4,S5). Moreover, the recognition motif of the DPAC-S@CB[7] were characterized in detail. It has been proved that cucurbit[7]uril can bond positively charged guest molecule.[16] The end of DPAC-S has pyridine group with positive charge. The cavity of one CB[7] molecule accommodate just one pyridine derivative. Job's plot confirmed that DPAC-S@CB[7] complexes adopted a 1:1 stoichiometry ostensibly, which means the binding motif of DPAC-S@CB[7] complexes should be a simply 1:1 binding motif (Figure S6, 7). Furthermore, on the basis of the UV/Vis absorbance titration, the association constants (K_a) could be calculated as (6.257 ± 0.667) $\times 10^4$ L mol^{-1} for DPAC-S@CB[7] using a nonlinear least-squares curve-fitting method (Figure S8). Fluorescence titration showed that the fluorescence of DPAC-S increased obviously with the addition of CB[7], and there was a slight blue shift due to the steric hindrance of the CB[7] to the vibration-induced emission (VIE) molecules DPAC-S (Figure S9), which further confirmed the assembly effect between host and guest.[17]

The hydrophobic layer of the assembly can effectively load water-insoluble substances. Nanoparticles with chemiluminescence properties are prepared by co-assembly of CPPO and DPAC-S@CB[7]. The loading of CPPO on the assembly was demonstrated by measuring the transmittance of the mixture aqueous solution (Figure S10). The THF solution containing CPPO was dripped into the aqueous solution containing the assembly. After ultrasound treatment, the transmittance of the solution was tested. With the addition of CPPO, the transmittance of solution decreases slowly. However, the amount of CPPO increases to 30 μL, transmittance of solution decreases sharply. We speculated that load capacity of the assembly for CPPO reaches its limit at this time and the resulting nanoparticles was named as DPAC-S@CB[7]@CPPO. Furthermore, SEM and TEM results confirm that nano-assembly has spherical morphology (Figure 1(a, b)). Dynamic light scattering (DLS) results show that the DPAC-S@CB[7]@CPPO can spontaneously form nano-sized aggregates with comparable size of the average hydrodynamic diameter of ~285 nm (Figure 1(c)). There is no accurate data to determine whether the nanoparticles are solid or hollow. Tests of Zeta potential gave an average zeta potential of the DPAC-S@CB[7]@CPPO of +42.2 mV (Figure 1(d)), which means that DPAC-S@CB[7]@CPPO have the potential to target mitochondria.[15] The stability of DPAC-S@CB[7]@CPPO in the in RPMI 1640 culture medium was assessed by detecting the change of UV absorption spectrum (Figure S11). The results show that DPAC-S@CB[7]@CPPO remains unchanged during the test, indicating that they have good stability.

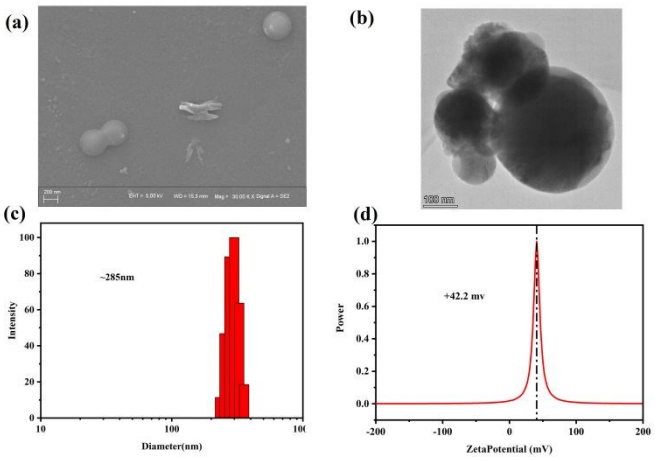

Figure 1. (a) The SEM of the DPAC-S@CB[7]@CPPO assembly in water; (b) TEM of the DPAC-S@CB[7]@CPPO assembly in water; (c) DLS of the DPAC-S@CB[7]@CPPO assembly in water; (d) Zeta potential of the DPAC-S@CB[7]@CPPO assembly in water.

The chemiluminescence of DPAC-S@CB[7]@CPPO stimulated by H_2O_2 was verified by naked eye and fluorescence spectroscopy. After the addition of excessive H_2O_2, the DPAC-S@CB[7]@CPPO emits yellow fluorescence immediately and the spectrum of chemiluminescence is almost the same as that of fluorescence (Figure 2(a)). This phenomenon means that the energy produced by the reaction of CPPO with H_2O_2 in nanoparticles can be effectively

absorbed by DPAC-S. Thanks to the good water solubility of DPAC-S@CB[7]@CPPO in aqueous solution, H_2O_2 can quickly diffuse into the assembly and react with CPPO. As shown in Figure 2(b), the maximum intensity of chemiluminescence can be achieved in only two minutes, which means DPAC-S@CB[7]@CPPO have a rapid response to H_2O_2. Moreover, when the concentration of H_2O_2 in solution is 1 mM, the chemiluminescence signal can be captured by IVIS lumina in vivo imaging system (Figure S12). This result enables the DPAC-S@CB[7]@CPPO to have the potential to diagnose and localize tumors.

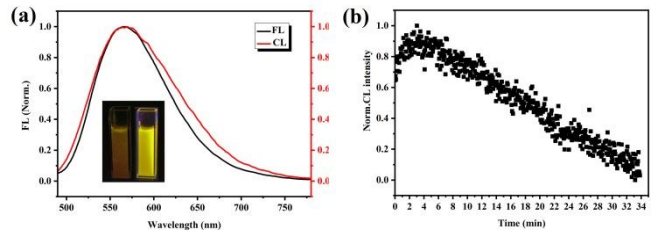

Figure 2. (a) Chemiluminescence (CL) and fluorescence (FL) spectra of DPAC-S@CB[7]@CPPO. The inset shows photographs of the CL and FL of assemblies; (b) Changes of chemiluminescence intensity with time.

To confirm that DPAC-S@CB[7]@CPPO can produce $^1O_2$ under light radiation, 9, 10-anthracenediyl-bis (methylene) dimalonic acid (ABDA) was used as a $^1O_2$ probe to evaluate the ability of DPAC-S@CB[7]@CPPO to produce $^1O_2$ by UV-vis spectroscopy.[18] In addition, the rose bengal (RB) was used as a control to further calculate the $^1O_2$ quantum yield of the assembly. It can be seen from Figure 3(a), when DPAC-S@CB[7]@CPPO and ABDA are in the solution at the same time, the UV absorption of ABDA at 378 nm decreases with the increase of illumination time, indicating that the assembly is an effective photosensitizer. The $^1O_2$ quantum yield of the assembly can be calculated to be 0.54 by Eq.1 with rose Bengal (RB) as the control (Figure 3d-f). Moreover, the ability of DPAC-S@CB[7]@CPPO to generate chemiexcited $^1O_2$ was also qualitatively evaluated. As shown in Figure S13, the mixture of CPPO and H_2O_2 was used as a blank sample and gave little effect on the degradation of ABDA. However, activated by H_2O_2, DPAC-S@CB[7]@CPPO can easily degrade ABDA and the absorption of ABDA is inversely proportional to the chemiluminescence time of the DPAC-S@CB[7]@CPPO. Furthermore, TEMPO (2,2,6,6-tetramethylpiperidine 1-oxyl) was used as $^1O_2$ trapping agent to effectively capture paramagnetic signals of $^1O_2$ by blending TEMPO with H_2O_2 and DPAC-S@CB[7]@CPPO under dark conditions (Figure S13 (d)). These results confirm that DPAC-S@CB[7]@CPPO can produce efficiently $^1O_2$ through chemiluminescence process. According to the above test results, it is inferred that the process of $^1O_2$ generation by chemiluminescence is as follows. CPPO has a unique response process to H_2O_2, because it can be decomposed by H_2O_2 to form a high-energy 1, 2-dioxetanedione transition state. Through a chemically initiated electron exchange luminescence (CIEEL) process, nearby fluorescent molecules can be excited.[19] Therefore, after contact with H_2O_2, DPAC-S was stimulated by CIEEL process to produce chemiluminescence in DPAC-S@CB[7]@CPPO. Meanwhile, excited DPAC-S reacts with oxygen to produce $^1O_2$ through intersystem crossing (ISC) from singlet (S1) to triple (T1) excited states. To sum up, DPAC-S@CB[7]@CPPO has great potential for PDT without external illumination.

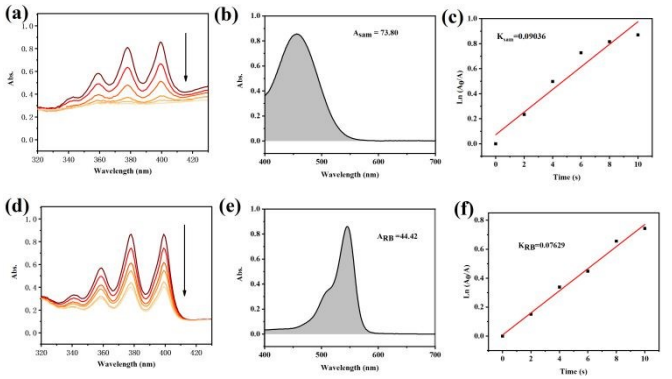

Figure 3. Measurement of quantum yield of $^1O_2$. (a) ABDA captures the UV-Vis spectrum of $^1O_2$ in the presence of DPAC-S@CB[7]@CPPO; (b) DPAC-S@CB[7]@CPPO absorption peak area;(c) ABDA decomposition rate constant by DPAC-S@CB[7]@CPPO (d) ABDA captures the UV-Vis spectrum of $^1O_2$ In the presence of RB. (e) RB absorption peak area; (f) ABDA decomposition rate constant by RB.

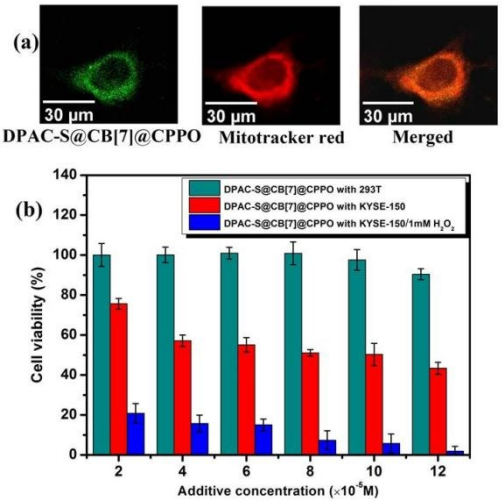

Figure 4. (a) Confocal fluorescence images of KYSE-150 cells after incubation with DPAC-S@CB[7]@CPPO for 24 h (scale bar=30μm); (b) Toxicity of DPAC-S@CB[7]@CPPO to different cells, 293T (dark cyan bar), KYSE-150 cell (red bar), KYSE-150 cell with 1mM H_2O_2 (blue bar).

Then, we assessed the cell uptake of DPAC-S@CB[7]@CPPO and DPAC-S@CPPO by laser confocal microscopy. The fluorescence of DPAC-S@CB[7]@CPPO was clearly observed in KYSE-150 cells after 24 hours of incubation (Figure S14). However, DPAC-S@CPPO cannot be swallowed by cells due to its large size of volume. Further, since the surface of the DPAC-S@CB[7]@CPPO is full of positive charges and the membrane potential on the surface of mitochondrial membrane is negative.[15] The DPAC-S@CB[7]@CPPO has the ability to locate at mitochondria. To verify this hypothesis, mitotracker red were used to stain the cell. As shown in Figure 4a, the DPAC-S@CB[7]@CPPO localized preferentially at mitochondria in KYSE-150 cells (the Pearson's correlation and overlap coefficient are shown in Figure S15). To exclude the localization of this nanoparticle in other organelles, such as lysosome, a subcellular co-localization study of DPAC-S@CB[7]@CPPO with lysosome was also carried out, showing that the DPAC-S@CB[7]@CPPO could not effectively localize at lysosome (Figure S16). Moreover, mitochondria are one of the main organelles that produce H_2O_2 in cells.[20] Mitochondrial targeting facilitates the PDT and chemiluminescence processes of H_2O_2-activated DPAC-S@CB[7]@CPPO, which is more conducive to the implementation of

the therapeutic effect of the DPAC-S@CB[7]@CPPO. In addition, because mitochondria are more susceptible to $^1O_2$ damage than other organelles, mitochondrial-targeted DPAC-S@CB[7]@CPPO can maximize PDT outcome. [21]

The viability of 293T and KYSE-150 cells treated with DPAC-S@CB[7]@CPPO was assessed by CCK8.[22] Two types of cell lines (KYSE-150 and 293T) were use to evaluate the cytotoxic effects of DPAC-S@CB[7]@CPPO at a cellular level (Figure 4b). Under dark conditions, the DPAC-S@CB[7]@CPPO was incubated with KYSE-150 and 293T for 24 hours, respectively. The incubation of DPAC-S@CB[7]@CPPO with 293T cells revealed that the cell viability remained around 100% throughout the incubation period, indicating that DPAC-S@CB[7]@CPPO was nontoxic to the normal cell. However, the cell toxicity to KYSE-150 increased with increase of the concentration of the DPAC-S@CB[7]@CPPO. It speculates that the different toxicity of assemblies to two types of cells is related to the concentration of H_2O_2 produced in the physiological process of cells. Tumor cells can rapidly produce a large amount of H_2O_2, which enables DPAC-S@CB[7]@CPPO to effectively produce chemiluminescence and PDT effects.[23] Furthermore, by adding 1 mM H_2O_2 to simulate the microenvironment of tumor tissues, the cytotoxicity of the assembly was further enhanced by H_2O_2, which means that therapeutic effect of the DPAC-S@CB[7]@CPPO is positively correlated with the concentration of H_2O_2 in the tumor. These phenomena indicate that the assembly has specific toxicity to cancer cells, which makes the assembly have a greater application prospect as a treatment of cancer.

In conclusion, we have successfully constructed mitochondrial-targeted chemiluminescent supramolecular assembly for in situ PDT through photosensitizer DPAC-S, macrocyclic molecule CB[7] and CPPO. The good water solubility and biocompatibility of the assembly enable it to enter cells. In addition, positive charges on the surface of the assembly give it the ability to target mitochondria. Mitochondrial H_2O_2 can rapidly activate CPPO molecules to generate energy after entering cancer cells and its energy can be effectively absorbed by nearby DPAC-S to lead chemiluminescence and $^1O_2$ generation in suit to kill cancer cells. The results show that the PDT effect produced by chemiluminescent supramolecular assembly is specific to cancer cells. This work effectively solves the dependence of traditional PDT on external light source, and provides an effective reference for the treatment of deep tissue tumors.

We thank NNSFC (Nos. 21672113, 21772099, 21861132001 and 21971127) for financial support.

Conflicts of interest

There are no conflicts to declare.

Notes and references

[1] a) C. Ji, Q. Gao, X. Dong, W. Yin, Z. Gu, Z. Gan, Y. Zhao and M. Yin, *Angew. Chem., Int. Ed.* 2018, **57**, 11384; b) C. Qian, J. Yu, Y. Chen, Q. Hu, X. Xiao, W. Sun, C. Wang, P. Feng, Q. D. Shen and Z. Gu, *Adv. Mater.* 2016, **28**, 3313; c) M. Yang, T. Yang and C. Mao, *Angew. Chem., Int. Ed.* 2019, **58**, 14066; (d) X. Li, S. Lee, J. Yoon ,*Chem. Soc. Rev.* 2018, **47**, 1174; (e) X.. Li, Yu. S, Lee, J. Yoon, *J. Am. Chem. Soc.* 2018, **141**, 1366; (f) X. Li, S .Yu, D. Lee, *ACS Nano*, 2018, **12,** 681; (g) X. Li, H. Bai, Y. Yang, *Adv. Mater.* 2019, **31**, 1805092; (h) Z. H. Yu, X. Li, F. Xu, *Angew. Chem., Int. Ed,* 2020, **59**, 3658; (i) H. B. Cheng, X. Li, N. Kwon, *Chem. Commun*. 2019, **55**, 12316.

[2] a) S. Chakrabortty, B. K. Agrawalla, A. Stumper, N. M. Vegi, S. Fischer, C. Reichardt, M. Kogler, B. Dietzek, M. Feuring-Buske, C. Buske, S. Rau and T. Weil, *J. Am. Chem. Soc.* 2017, **139**, 2512; b) N. Cheng, Y. Chen, J. Yu, J. J. Li and Y. Liu, *Bioconjugate Chem*. 2018, **29**, 1829.

[3] Á. Juarranz, P. Jaén, F. Sanz-Rodríguez, J. Cuevas and S. González, *Clin. Transl. Oncol.* 2008, **10**, 148.

[4] a) M. Ethirajan, Y. Chen, P. Joshi and R. K. Pandey, *Chem. Soc. Rev.* 2011, **40**, 340; b) G. Gollavelli and Y. C. Ling, *Biomaterials* 2014, **35**, 4499.

[5] H. Chen, J. Zhang, K. Chang, X. Men, X. Fang, L. Zhou, D. Li, D. Gao, S. Yin, X. Zhang, Z. Yuan and C. Wu, *Biomaterials* 2017, **144**, 42.

[6] J. M. Baumes, J. J. Gassensmith, J. Giblin, J.-J. Lee, A. G. White, W. J. Culligan, W. M. Leevy, M. Kuno and B. D. Smith, *Nat. Chem.* 2010, **2**, 1025.

[7] a) D. Lee, S. Khaja, J. C. Velasquez-Castano, M. Dasari, C. Sun, J. Petros, W. R. Taylor and N. Murthy, *Nat. Mater.* 2007, **6**, 765; b) A. J. Shuhendler, K. Pu, L. Cui, J. P. Uetrecht and J. Rao, *Nat. Biotechnol.* 2014, **32**, 373.

[8] a) A. Jezierska-Drutel, S. A. Rosenzweig and C. A. Neumann, *Adv. Cancer. Res*. 2013, **119**, 107; b) H. Yuan, H. Chong, B. Wang, C. Zhu, L. Liu, Q. Yang, F. Lv and S. Wang, *J. Am. Chem. Soc.* 2012, **134**, 13184.

[9] D. Mao, W. Wu, S. Ji, C. Chen, F. Hu, D. Kong, D. Ding and B. Liu, *Chem* 2017, **3**, 991.

[10] H.B. Cheng, Y.M. Zhang, Y. Liu and J. Yoon, *Chem*, 2019, **5**, 553.

[11] W. Chen, C. L. Chen, Z. Zhang, Y. A. Chen, W. C. Chao, J. Su, H. Tian, P. T. Chou, J. Am. Chem. Soc. 2017, 139, 1636-1644.

[12] a) J. J. Li, H. Y. Zhang, Y. Zhang, W. L. Zhou and Y. Liu, *Adv. Opt. Mater*. 2019, 1900589; b) Y. M. Zhang, J. H. Liu, Q. Yu, X. Wen and Y. Liu, *Angew. Chem., Int. Ed.* 2019, **58**, 10553; c) Y. M. Zhang, Y. H. Liu and Y. Liu, *Adv. Mater*. 2019, **37**,843.

[13] J. J. Li, Y. Chen, J. Yu, N. Cheng and Y. Liu, *Adv. Mater.* 2017, **29**, 1701905.

[14] a) X. Guan, Y. Chen, X. Wu, P. Li and Y. Liu, *Chem. Commun*. 2019, **55**, 953; b) J. H. Liu, X. Wu, Y. M. Zhang and Y. Liu, *Asian. J. Org. Chem.* 2018, **7**, 2444.

[15] M. Li, S. Long, Y. Kang, L. Guo, J. Wang, J. Fan, J. Du and X. Peng, *J. Am. Chem. Soc.* 2018, **140**, 15820.

[16] a) H. Wu, Y. Chen, X. Dai, P. Li, J. F. Stoddart and Y. Liu, *J. Am. Chem. Soc.* 2019, **141**, 6583; b) Z. Y. Zhang, Y. Chen and Y. Liu, *Angew. Chem., Int. Ed*. 2019, **58**, 6028; c) X. M. Chen, Y. Chen, Q. Yu, B. H. Gu and Y. Liu, *Angew. Chem., Int. Ed.* 2018, **57**, 12519.

[17] a) J. Wang, X. Yao, Y. Liu, H. Zhou, W. Chen, G. Sun, J. Su, X. Ma and H. Tian, *Adv. Opt. Mater*. 2018, **6**, 1800074; b) Z. Zhang, C. L. Chen, Y. A. Chen, Y. C. Wei, J. Su, H. Tian and P. T. Chou, *Angew. Chem., Int. Ed.* 2018, **57**, 9880.

[18] H.P. Tham, H. Chen, Y. H. Tan, *Chem. Commun.* 2016, **52**: 8854.

[19] Y. D. Lee, C. K. Lim, A. Singh, J. Koh, J. Kim, I. C. Kwon and S. Kim, *ACS .Nano.* 2012, **6**, 6759.

[20] K. Xu, M. Qiang, W. Gao, R. Su, N. Li, Y. Gao, Y. Xie, F. Kong and B. Tang, *Chem. Sci*. 2013, **4**, 1079.

[21] W. Lv, Z. Zhang, K. Y. Zhang, H. Yang, S. Liu, A. Xu, S. Guo, Q. Zhao and W. Huang, *Angew. Chem., Int. Ed.* 2016, **55**, 9947.

[22] Q. Yu, Y.-M. Zhang, Y.-H. Liu, X. Xu and Y. Liu, *Sci. Adv.* 2018, **4**, eaat2297.

[23] T. P. Szatrowski, C. F. Nathan, *Cancer. Res.* 1991, **51**, 794.